Classical Antiferromagnetism in Kinetically Frustrated Electronic Models

C. N. Sposetti, B. Bravo, A. E. Trumper, C. J. Gazza, and L. O. Manuel
Instituto de Física Rosario (CONICET) and Universidad Nacional de Rosario, Boulevard 27 de Febrero 210 bis, (2000) Rosario, Argentina

(Received 23 December 2013; revised manuscript received 28 February 2014; published 9 May 2014)

We study, by means of the density matrix renormalization group, the infinite U Hubbard model—with one hole doped away from half filling—in triangular and square lattices with frustrated hoppings, which invalidate Nagaoka's theorem. We find that these kinetically frustrated models have antiferromagnetic ground states with classical local magnetization in the thermodynamic limit. We identify the mechanism of this kinetic antiferromagnetism with the release of the kinetic energy frustration, as the hole moves in the established antiferromagnetic background. This release can occur in two different ways: by a nontrivial spin Berry phase acquired by the hole, or by the effective vanishing of the hopping amplitude along the frustrating loops.

DOI: 10.1103/PhysRevLett.112.187204 PACS numbers: 75.10.Lp, 71.10.Fd

Itinerant magnetism has proven to be an elusive subject in condensed matter physics, since itinerant and localized aspects of electrons need to be taken into account on an equal footing. The single-band Hubbard model, originally proposed to describe metallic ferromagnetism [1], has also been associated with the antiferromagnetism of kinetic exchange origin close to half filling. While *virtual* kinetic processes favor antiferromagnetism, it is a rule of thumb to link *real* kinetic processes with ferromagnetism [2]. However, there exist only few exact results that ensure the existence of itinerant ferromagnetism [3,4]. Among these, the most renowned is Nagaoka's theorem [3], which asserts that the saturated ferromagnetic state is the unique ground state when one hole is doped on the half-filled Hubbard model with infinite U Coulomb repulsion. Furthermore, a connectivity condition must be fulfilled for the validity of Nagaoka's theorem: The sign of the hopping amplitudes around the smallest closed loop of the lattice must be positive, otherwise the hole kinetic energy will be frustrated and the saturated ferromagnetic state will no longer be the ground state. Kinetic energy frustration is a quantum mechanical phenomenon without a classical analog, easily understood in certain tight-binding models where an electron cannot gain the full kinetic energy $-z|t|$ because of quantum interferences [5,6]. This kind of frustration has been considerably less studied than the magnetic one, although recent works indicate that its effects may lead to rich physics, such as robust superconductivity in a strongly repulsive fermionic system [7] and spontaneous time-reversal symmetry breakings [8], among others [9,10].

In a seminal work, Haerter and Shastry [11] have found a 120° antiferromagnetic Néel order as the ground state of the $U = \infty$ triangular lattice Hubbard model when the hole motion is frustrated ($t > 0$), thus uncovering a new mechanism for itinerant magnetism. In this Letter, we further characterize this kinetic antiferromagnetism; we describe its microscopic origin, analyzing generic kinetically frustrated electronic models for which, in the limit of infinite Coulomb repulsion and one hole doped away from half filling, Nagaoka's theorem is not valid. In particular, we study the ground state of two Hubbard models: one on the triangular lattice with a positive hopping term, and the other on the square lattice with a positive second-neighbor hopping term. Using the density matrix renormalization group (DMRG) [12,13], we find in both cases that the ground state has an antiferromagnetic order: a 120° Néel order for the triangular lattice and the usual (π, π) Néel order for the square lattice. Surprisingly, we find that the local staggered magnetization becomes classical (saturated) in the thermodynamic limit. This result can be thought as the almost-perfect antiferromagnetic counterpart of the Nagaoka ferromagnetism; the difference is that, as the local staggered magnetization does not commute with the $SU(2)$ invariant Hubbard Hamiltonian, classical antiferromagnetic states cannot be the exact eigenvectors for finite lattices. Based on a simple slave-fermion mean field [14], we propose a mechanism responsible for the kinetic antiferromagnetism: If the hole were moving on a ferromagnetic background on these lattices, its kinetic energy would be frustrated. However, when moving on a certain antiferromagnetic background, the hole can release its kinetic energy frustration by (depending on the system) acquiring a nontrivial spin Berry phase or having zero hopping amplitude along frustrating loops. As the Coulomb repulsion is infinite, no exchange interaction exists, thus the stabilization of the antiferromagnetism is purely of kinetic origin.

Hubbard model and DMRG.—We study the Hubbard model, $H = -\sum_{\langle ij\rangle\sigma} t_{ij}(\hat{c}^{\dagger}_{i\sigma}\hat{c}_{j\sigma} + \text{H.c.}) + U\sum_i \hat{n}_{i\uparrow}\hat{n}_{i\downarrow}$, where we use the usual notation, and $\langle ij\rangle$ denotes pairs of neighbor sites connected by the hopping parameters t_{ij}. From the outset, we take $U = \infty$. We study the Hubbard

model on two lattices with frustrated kinetic hole energy: the triangular lattice with positive t and the square lattice with nearest t_1 and positive next-nearest neighbor t_2 hopping terms. In the latter case, we choose $t_2 = t_1 > 0$ as a generic point with kinetic frustration. We take $t = t_1 = 1$ as the energy unit.

To solve the Hubbard model we apply DMRG on ladders of dimension $L_x \times L_y$ (see Fig. 1 in [15]), with up to $L_y = 6$ legs and $L_x = 15$ rungs. We choose clusters that are compatible with the antiferromagnetic orders found in this Letter. This means that we take an even number of legs, L_y, for both lattices, and an even (multiple of 3) L_x for the square (triangular) lattice. We consider cylindrical boundary conditions with periodic wrapping in the rung direction and open boundary conditions along the legs. Comparing results obtained with clusters of different numbers of legs, we find that the clusters with $L_y = 6$ give a correct description of the two-dimensional systems. A similar conclusion has been reached previously on square ladders [16]. We have kept the truncation error less than $O(10^{-7})$, ensuring that errors of the DMRG are smaller than symbol sizes in each figure.

We have also considered the inclusion of a weak pinning magnetic field ($B = 0.1t$) acting on only a single site, at the lower left-hand end of the clusters [16] or on one magnetic sublattice. In previous works [12], the purpose of the small magnetic field has been to pin a possible magnetic order for the purpose of reducing the computational efforts, by computing the average value of the local spin instead of correlation functions, thereby optimizing the truncation error. In our Letter, the inclusion of the weak magnetic field will allow us to highlight the classical character of the ground states.

Static magnetic structure factor.—To detect the existence of magnetic order, we compute the static magnetic structure factor with DMRG for both lattices, $S^{zz}(\mathbf{k}) = (1/N)\sum_{ij}\langle S_i^z \cdot S_j^z\rangle e^{-i\mathbf{k}(\mathbf{r}_i - \mathbf{r}_j)}$, where $N = L_x L_y$ is the number of sites in the cluster, and i, j run over all sites. In the inset of Fig. 1(a) we show an intensity plot of $S^{zz}(\mathbf{k})$ for a triangular cluster with $L_y = 6$ legs and $N = 90$ sites. For positive t, $S^{zz}(\mathbf{k})$ exhibits two sharp maxima at the momenta $\mathbf{Q} = (4\pi/3, 0)$ and $\mathbf{Q}^* = (2\pi/3, 2\pi/\sqrt{3})$, corresponding to a three-sublattice 120° Néel order. As these peaks diverge with increasing cluster size, the ground state exhibits a long-range magnetic order of 120° . Haerter and Shastry [11] previously obtained this result by diagonalizing the corresponding effective spin Hamiltonian on smaller clusters (up to 27 sites). Note that because we are working in the extremely correlated limit, where the exchange interaction driven by *virtual* kinetic processes vanishes, $J = 0$, the magnetic order can only have its origin in the hole motion. On the other hand, as the triangular Heisenberg model has the same 120° Néel order in its ground state [17,18], for finite U ($J > 0$) and low doping, there is a synergy between *real* and *virtual* kinetic processes which leads to the strengthening of the 120° Néel order with respect to the half-filled case [19,20].

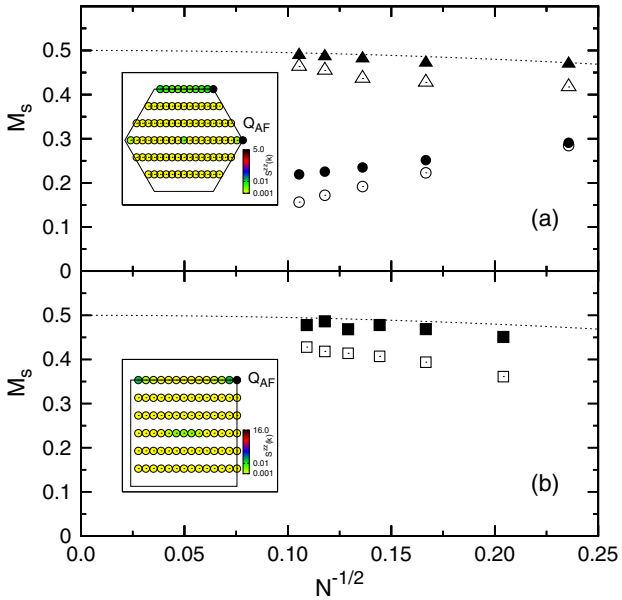

FIG. 1 (color online). Local magnetization versus $1/\sqrt{N}$ for (a) $U = \infty$ triangular Hubbard (triangles) and Heisenberg (circles) models, without a magnetic field (open symbols) and with a magnetic field $B = 0.1t$ applied to one sublattice (solid symbols); (b) $U = \infty$ square Hubbard model with first- and second-neighbor hopping terms ($t_1 = t_2 = 1$), without a magnetic field (open squares) and with a magnetic field $B = 0.1t_1$ applied to one sublattice (solid squares). Dashed lines represent classical local magnetization. Insets: Intensity plot $S^{zz}(\mathbf{k})$ for the (a) triangular and (b) square models. Darker color indicates a larger magnetic structure factor. $\mathbf{Q}_{\mathrm{AF}} = (4\pi/3, 0)$ and (π, π) for the triangular and square lattice, respectively.

For negative t (not shown in the figure), the magnetic structure factor has a sharp peak at $\mathbf{k} = 0$, while it vanishes for all other momenta. This result corresponds to a fully polarized ferromagnetic ground state, as predicted by Nagaoka's theorem.

In the inset of Fig. 1(b) we show the magnetic structure factor for the $U = \infty$ Hubbard model on square clusters with $L_y = 6$ legs and $N = 84$ sites, for $t_2 = t_1 > 0$. Here, there is a marked peak for the magnetic wave vector $\mathbf{Q} = (\pi, \pi)$, corresponding to the usual two-sublattice Néel order. If we relax the infinite U condition, the kinetic exchange interactions would favor a collinear antiferromagnetic order, characterized by the magnetic wave vector $(\pi, 0)$ or $(0, \pi)$; there would be a competition between *real* and *virtual* kinetic processes, resulting in magnetic incommensuration and phase separation [20]. For $t_2 < 0$, the ground state is the saturated ferromagnet, in agreement with Nagaoka's theorem.

Local magnetization.—After the magnetic structure factor has been computed, we can obtain the order parameter for the antiferromagnetic order, the local staggered magnetization $M_s = \sqrt{(1/N)\sum_\alpha \langle(\sum_{i\in\alpha} S_i)^2\rangle}$ [21], where α denotes the magnetic sublattices. The cluster-size dependence of M_s

for the $U = \infty$ triangular Hubbard model is shown in Fig. 1(a) (open triangles), along with the local magnetization of the triangular Heisenberg model (open circles) for comparison. The dashed line indicates the classical local magnetization, $M_{s,\mathrm{classic}} = \frac{1}{2} - (1/2N)$, corrected by the presence of the hole uniformly distributed (as is confirmed by the DMRG calculations). Surprisingly, M_s is very close to the classical value, even for small clusters, and it reaches this value in the thermodynamic limit ($L_y = 6$, $L_x \to \infty$). On the other hand, in the Heisenberg case, strong zero-point quantum fluctuations lead to a drastic reduction of M_s [18], and due to the quasi-one-dimensional character of the clusters, M_s extrapolates to 0 [12,15]. One possible reason for the classical character of the magnetic order is that the effective spin model, obtained after integrating the hole degree of freedom, contains effective long-range interactions (see Eq. 3 in Ref. [11]) that may favor the classical ordering, like in the Lieb-Mattis model [22].

As we can see in Fig. 1(a), M_s for finite-size clusters does not take exactly the classical value. The Hubbard Hamiltonian is $SU(2)$ spin-rotational invariant and does not commute with the antiferromagnetic order parameter; consequently, its ground state cannot break this symmetry for finite systems. Instead, it is expected that the finite-size ground state is a singlet, and only in the thermodynamic limit can there be a spontaneous $SU(2)$ symmetry breaking driven by the collapse of many low-lying states onto the ground state [17]. The existence of a tower of states for the $U = \infty$ triangular Hubbard model has been confirmed in Ref. [11]. We argue that the small departure of the order parameter from the classical value is related to the singlet character of the finite-size ground state, and not to zero-point quantum fluctuations that reduce the order parameter, as in quantum antiferromagnets. Pictorially, the finite-size ground state can be thought of as a linear combination of several classical antiferromagnetic states lying in different planes. To strengthen this picture, we apply a small uniform pinning magnetic field, $B = 0.1t$, in one sublattice only. (If we apply the magnetic field in only one site, the difference is quantitatively small, of only a few percent.) Figure 1(a) shows M_s for the Hubbard model with the magnetic field applied (solid triangles) and the same for the triangular Heisenberg model (solid circles). It can be seen that in the Hubbard model M_s becomes classical, because the magnetic field selects one of the classical orders that compose the finite-size ground state. On the other hand, the magnetic field increases M_s of the Heisenberg model, but strong zero-point quantum fluctuations remain.

Figure 1(b) shows M_s for the Hubbard model on the square lattice, with (solid squares) and without (open squares) an applied uniform magnetic field in one sublattice. The same behavior as the triangular case is found: The local magnetization is close to the classical values when $B = 0$; it is enough the application of a small $B = 0.1t$ to pin one classical magnetic ground state.

Energy scale.—For the triangular lattice, the extrapolated ground state energy is -4.178 ± 0.001, in agreement with the value obtained in [11] (-4.183 ± 0.005), while for the square lattice the extrapolated value is -4.848 ± 0.001. In order to quantify the energy scale of the kinetic antiferromagnetism, we match the effect of the hole motion to an effective nearest-neighbor antiferromagnetic Heisenberg interaction, J_{eff} [11,23], resulting in $J_{\mathrm{eff}} \simeq \Delta e \equiv (E_F - E_{AF})/N$; this is the energy difference per site between the fully polarized ferromagnetic state and the antiferromagnetic ground states. We have found that $J_{\mathrm{eff}} \simeq 1.15/N$ ($J_{\mathrm{eff}} \simeq 0.7/N$) for the triangular (square) lattice, for large N.

Release of the kinetic frustration.—Now we trace back the origin of the kinetic antiferromagnetism by means of a comprehensive mean-field approximation. To this end, we use the slave fermion–Schwinger boson representation of the projected electronic degree of freedom in the $t - J$ model, the strong-coupling limit of the Hubbard model. Here, we give a brief description of the mean-field approach (see Supplemental Material [24] for the details). In this representation, the projected electronic operator is written as $\tilde{c}_{i\sigma} = b^{\dagger}_{i\sigma} f_i$, a composition of a Schwinger boson $b_{i\sigma}$, which accounts for the spin degrees of freedom, and a spinless slave fermion f_i, which describes the charge sector. This representation is replaced in the $t - J$ Hamiltonian, resulting in $H_{t-J} = -\sum_{\langle ij \rangle} 2t_{ij} (\hat{F}_{ij} \hat{B}^{\dagger}_{ij} + \mathrm{H.c.}) + H_{\mathrm{bos}}$, where we have defined the $SU(2)$ invariant operator $\hat{B}^{\dagger}_{ij} = \frac{1}{2} \sum_{\sigma} b^{\dagger}_{i\sigma} b_{j\sigma}$ related to ferromagnetic correlations between sites i and j [25], while $\hat{F}_{ij} = f^{\dagger}_i f_j$ describes the hole-hopping amplitude. H_{bos} is a bosonic term that represents the spin fluctuations due to the Heisenberg term, and it vanishes when $J \to 0$ [14]. After a mean-field decoupling, we get $H^{\mathrm{MF}}_{t-J} = \sum_{\mathbf{k}} \varepsilon_{f\mathbf{k}} f^{\dagger}_{\mathbf{k}} f_{\mathbf{k}} + H^{\mathrm{MF}}_{\mathrm{bos}}$, where the hole kinetic energy dispersion takes the form $\varepsilon_{f\mathbf{k}} = 2 \sum_{\mathbf{R}} t_R B_R \cos \mathbf{k} \cdot \mathbf{R}$ ($\mathbf{R}$ are the relative position vectors of the sites connected by t_R). In the one-hole case, the ground-state energy of the system corresponds to the bottom of $\varepsilon_{f\mathbf{k}}$. This energy dispersion is tight-binding-like, with the hopping terms t_R renormalized by the ferromagnetic mean-field parameter B_R: $t_R \to t^{\mathrm{eff}}_R = t_R B_R$. The presence of the B parameters has two consequences: On one hand, the hopping terms are renormalized as in the double-exchange mechanism [26], $t^{\mathrm{eff}}_R \sim t_R \cos(\varphi_R/2)$, where φ_R is the angle between the spins separated by vector R; if the spins are antiparallel, t^{eff}_R vanishes. On the other hand, the renormalization can give rise to a nontrivial spin Berry phase for noncollinear orders, encoded in the B_R signs and associated with the solid angle subtended by the spins on a closed loop [24].

When the system is kinetically frustrated, these two features of the hopping renormalizations act, releasing the hole kinetic energy frustration as the hole moves through certain antiferromagnetic patterns. Now we describe how this release works in the triangular and square lattice cases.

In the triangular lattice, for the ferromagnetic state, all B parameters are equal to $S = 1/2$; consequently, the hole motion is frustrated for $t > 0$. On the other hand, in a 120° Néel order, the parameters $B_{(\pm 1,0)}$ become negative, while the others remain positive because $B_R \sim M_s \cos(\mathbf{QR}/2)$ [25]. These negative B's turn the hole dispersion upside down, releasing the kinetic frustration of the hole motion. Notice that the flux of the B parameters in a closed loop is the solid angle subtended by the magnetic order, and consequently it is associated with the spin Berry phase detected by the hole (see Supplemental Material [24] for details). In the square lattice case, when $t_2 > 0$, the hole motion in a ferromagnetic state is frustrated. However, in the (π, π) Néel order, the vanishing of the effective first-neighbor hopping terms (due to their antiparallel spins [26]) removes the frustrating loops, thus releasing the kinetic frustration.

We remark that, at the mean-field level, the 120° Néel [(π, π) Néel] state is degenerate with the ferromagnetic one in the triangular case with $t > 0$ (square lattice with $t_2 > 0$). The reason for this degeneracy is that, although the hole motion through the antiferromagnetic states is not frustrated, there is a hole dispersion bandwidth reduction due to the hopping renormalizations [24]. So, strictly speaking, the mean-field numerics do not show the stabilization of the kinetic antiferromagnetism over the Nagaoka state. However, after considering the combined effects of quantum interference and strong-correlation physics beyond the mean-field approximation (as in our DMRG predictions), the actual kinetic antiferromagnetism emerges. Despite the mean-field discrepancy, we strongly emphasize that the mean field approach allows us to find one of the main ingredients of the kinetic antiferromagnetism; that is, the release of the kinetic frustration.

Using the insight we gained from the mean-field approach, we can predict the appearance of this novel kinetic antiferromagnetism phenomenon in other kinetically frustrated systems, like the anisotropic triangular lattice and the $t_1 - t_2$ square lattice with $t_2 \neq |t_1|$. Preliminary DMRG results show the ubiquity of kinetic antiferromagnetism in these systems (see Supplemental Material [24]). Furthermore, we remark that the kinetic antiferromagnetism mechanism is completely different from the exchange one; in general, the ground state selected by this itinerant mechanism does not necessarily have to be the classical ground state of the related Heisenberg model. In this context, in particular, the $U = \infty$ kagome Hubbard model, with one hole doped and $t > 0$, may be a promising candidate for the search of unconventional kinetic antiferromagnetism physics [24].

Finally, if we lift the condition of infinite U, it is possible to study the synergy between *real* and *virtual* kinetic processes in order to highlight the crossover from the Heisenberg regime, governed by the exchange interactions, to the kinetic antiferromagnetic one, governed by the kinetic energy. In Fig. 2 we show the local magnetization

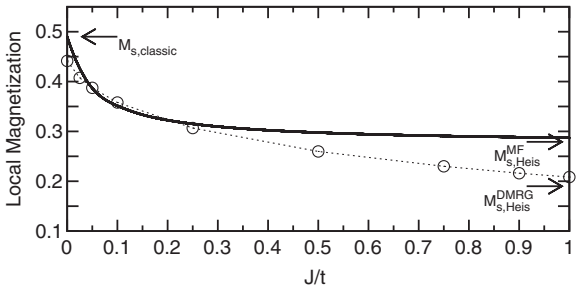

FIG. 2. Local magnetization M_s of the triangular $t - J$ model as a function of J/t for doping $\delta = 0.0185$. The solid line corresponds to the mean field M_s and the open circles to the DMRG results; the dashed line is to aid the eye. The arrows indicate the $J = 0$ and Heisenberg M_s limits.

of the ground-state 120° Néel order of the triangular $t - J$ model predicted by the mean-field approach and DMRG [27], as a function of J/t for doping $\delta = 0.0185$. There is fairly good qualitative agreement between both methods; for larger values of J/t the order parameter is close to the Heisenberg value calculated within each approach, $M^{\mathrm{MF}}_{s,\mathrm{Heis}} \sim 0.275$ [28] and $M^{\mathrm{DMRG}}_{s,\mathrm{Heis}} \sim 0.205$ [12], while M_s increases with decreasing J/t until it reaches the classical value for $J/t \to 0$ in both methods.

Conclusions.—Using the density matrix renormalization group, we find that classical antiferromagnetic ground states can be realized in extremely correlated electronic systems with frustrated kinetic energy. In particular, we study the $U = \infty$ Hubbard model, with one hole doped away from half filling, on the positive t triangular lattice, and on the square lattice with positive second-neighbor hoppings. We also propose a mechanism responsible for this kinetic antiferromagnetism, that is, the release of the kinetic energy frustration driven by (depending on the system) the spin Berry phase acquired by the hole while moving around an antiferromagnetic background, or the vanishing of the effective hopping amplitude along the frustrating loops. This new mechanism for itinerant antiferromagnetism is quite ubiquitous for one hole doped away from half filling in kinetically frustrated lattices [24]; it is also relevant in more general situations, like the finite U regime and low-doping cases, as the mean-field results seem to indicate [20]. It is worth noticing that recent experiments [29] were able to generate gauge fields that induced frustrated motion of ultracold bosons in triangular optical lattices, opening up the possibility to observe related kinetic antiferromagnetism phenomena.

We acknowledge useful discussions with C. D. Batista and D. J. García. This work was partially supported by PIP CONICET Grants No. 0160 and No. 0392.

[1] M. C. Gutzwiller, Phys. Rev. Lett. **10**, 159 (1963); J. Hubbard, Proc. R. Soc. A **276**, 238 (1963).
[2] P. Fazekas, *Electron Correlation and Magnetism* (World Scientific, Singapore, 1999).

[3] Y. Nagaoka, Phys. Rev. **147**, 392 (1966).
[4] A. Mielke, J. Phys. A **24**, 3311 (1991); H. Tasaki, Phys. Rev. Lett. **69**, 1608 (1992); Y. Saiga and M. Oshikawa, Phys. Rev. Lett. **96**, 036406 (2006).
[5] W. Barford and J. H. Kim, Phys. Rev. B **43**, 559 (1991).
[6] J. Merino, B. J. Powell, and R. H. McKenzie, Phys. Rev. B **73**, 235107 (2006).
[7] L. Isaev, G. Ortiz, and C. D. Batista, Phys. Rev. Lett. **105**, 187002 (2010).
[8] O. Tieleman, O. Dutta, M. Lewenstein, and A. Eckardt, Phys. Rev. Lett. **110**, 096405 (2013).
[9] Y. F. Wang, C. D. Gong, and Z. D. Wang, Phys. Rev. Lett. **100**, 037202 (2008).
[10] Z. P. Yin, K. Haule, and G. Kotliar, Nat. Mater. **10**, 932 (2011).
[11] J. O. Haerter and B. S. Shastry, Phys. Rev. Lett. **95**, 087202 (2005).
[12] S. R. White and A. L. Chernyshev, Phys. Rev. Lett. **99**, 127004 (2007).
[13] S. R. White and I. Affleck, Phys. Rev. B **64**, 024411 (2001).
[14] L. O. Manuel and H. A. Ceccatto, Phys. Rev. B **61**, 3470 (2000).
[15] A. Weichselbaum and S. R. White, Phys. Rev. B **84**, 245130 (2011).
[16] L. Liu, H. Yao, E. Berg, S. R. White, and S. A. Kivelson, Phys. Rev. Lett. **108**, 126406 (2012).
[17] B. Bernu, P. Lecheminant, C. Lhuillier, and L. Pierre, Phys. Rev. B **50**, 10048 (1994).
[18] L. Capriotti, A. E. Trumper, and S. Sorella, Phys. Rev. Lett. **82**, 3899 (1999).
[19] C. Weber, A. Laeuchli, F. Mila, and T. Giamarchi, Phys. Rev. B **73**, 014519 (2006).
[20] C. N. Sposetti, A. Mezio, A. E. Trumper, C. J. Gazza, and L. O. Manuel (to be published).
[21] The expressions are $M_s = \sqrt{[4S^{zz}(\mathbf{Q})]/N}$ and $M_s = \sqrt{[S^{zz}(\mathbf{Q})]/N}$ for the triangular and square lattices, respectively.
[22] E. Lieb and D. Mattis, J. Math. Phys. (N.Y.) **3**, 749 (1962).
[23] J. O. Haerter, M. R. Peterson, and B. S. Shastry, Phys. Rev. B **74**, 245118 (2006).
[24] See Supplemental Material at http://link.aps.org/supplemental/10.1103/PhysRevLett.112.187204 for a complete description of the mean-field approximation and its results.
[25] H. A. Ceccatto, C. J. Gazza, and A. E. Trumper, Phys. Rev. B **47**, 12329 (1993).
[26] C. Zener, Phys. Rev. **82**, 403 (1951); P. W. Anderson and H. Hasegawa, Phys. Rev. **100**, 675 (1955).
[27] To compare similar results between the mean field M_s computed for the two-dimensional triangular lattice and DMRG computations done in clusters with $L_y = 6$ legs, we use the prescription given in Ref. [12] for choosing the optimal cluster shapes. In the case of 6 legs, this cluster is the 9×6 ladder.
[28] C. J. Gazza and H. A. Ceccatto, J. Phys. Condens. Matter **5**, L135 (1993).
[29] A. Eckardt, P. Hauke, P. Soltan-Panahi, C. Becker, K. Sengstock, and M. Lewenstein, Europhys. Lett. **89**, 10010 (2010); J. Struck, C. Ölschläger, R. L. Targat, P. Soltan-Panahi, A. Eckardt, M. Lewenstein, P. Windpassinger, and K. Sengstock, Science **333**, 996 (2011).